Transcellular Transport of Polymeric IgA in the Rat Hepatocyte: Biochemical and Morphological Characterization of the Transport Pathway

CRAIG A. HOPPE, TIMOTHY P. CONNOLLY, and ANN L. HUBBARD
Department of Cell Biology and Anatomy, Johns Hopkins University School of Medicine, Baltimore, Maryland 21205

ABSTRACT Polymeric IgA (pIgA) is transported by liver parenchymal cells (hepatocytes) from blood to bile via a receptor-mediated process. We have studied the intracellular pathway taken by a TEPC15 mouse myeloma pIgA. When from 1 μg to 1 mg ^{125}I-pIgA was injected into the saphenous vein of a rat, 36% was transported as intact protein into the bile over a 3-h period. The concentration of transported ^{125}I-pIgA was maximal in bile 30–60 min after injection, and ~80% of the total ^{125}I-pIgA ultimately transported had been secreted into bile by 90 min. A horseradish peroxidase-pIgA conjugate (^{125}I-pIgA-HRP) was transported to a similar extent and with kinetics similar to that of unconjugated ^{125}I-pIgA and was therefore used to visualize the transport pathway. Peroxidase cytochemistry of livers fixed in situ 2.5 to 10 min after ^{125}I-pIgA-HRP injection demonstrated a progressive redistribution of labeled structures from the sinusoidal area to intermediate and bile canalicular regions of the hepatocyte cytoplasm. Although conjugate-containing structures began accumulating in the bile canalicular region at these early times, no conjugate was present in bile until 20 min. From 7.5 to 45 min after injection ~30% of the labeled structures were in regions that contained Golgi complexes and lysosomes; however, we found no evidence that either organelle contained ^{125}I-pIgA-HRP. At least 85% of all positive structures in the hepatocyte were vesicles of 110–160-nm median diameters, with the remaining structures accounted for by tubules and multivesicular bodies. Vesicles in the bile canalicular region tended to be larger than those in the sinusoidal region. Serial sectioning showed that the ^{125}I-pIgA-HRP-containing structures were relatively simple (predominantly vesicular) and that extensive interconnections did not exist between structures in the sinusoidal and bile canalicular regions.

Receptor-mediated endocytosis is an important cellular process by which macromolecules enter cells. Liver parenchymal cells (hepatocytes) internalize a wide variety of molecules from the circulation via this mechanism; however, once endocytosed, the ligands exhibit diverse intracellular fates. Asialoglycoproteins (41) and epidermal growth factor (6) are taken up by rat hepatocytes and degraded in lysosomes, whereas polymeric IgA (pIgA)[1] is transported from blood to bile without degradation (24, 27, 30, 40). The fates of the surface receptors can also vary in hepatocytes. The asialoglycoprotein receptor is reutilized for further rounds of ligand internalization (33, 38), whereas the receptor for epidermal growth factor is degraded when cells are exposed to the hormone (6a). Secretory component (SC), the receptor for pIgA, is transported across the cell and secreted with its ligand as a complex (7, 16, 17).

Most of the pIgA that is transported from blood to bile in the liver is synthesized by plasma cells found in the lamina propria of the intestinal mucosa and enters the bloodstream at the thoracic duct (15). Circulating pIgA is then bound at the sinusoidal front of hepatocytes and transported across the

[1] *Abbreviations used in this paper:* HRP, horseradish peroxidase; PC_{25}-BSA-Sepharose 4B, Sepharose 4B to which 2.9 mg phosphorylcholine^{25}-bovine serum albumin per ml is attached; pIgA, polymeric ^{125}IgA; ^{125}I-pIgA-HRP, conjugate between pIgA and HRP; SC, secretory component; TBS, Tris-HCl-buffered saline.

cell, processes mediated by SC, a pIgA-specific receptor synthesized in the hepatocyte (7, 17, 23, 31, 34–36). During transport of the SC-pIgA complex across epithelial cells, the membrane-anchoring domain (20–36 kD) of the transmembrane receptor is cleaved (20, 32, 34). Morphological and biochemical studies have suggested that pIgA is transported across the hepatocyte within small vesicles (21, 27, 37). Another view has been put forward by Geuze et al., who reported that pIgA and asialofetuin, a ligand for the asialoglycoprotein receptor, are segregated from each other in a tubule network (compartment of uncoupling of receptors and ligand) that extends from the sinusoidal cell periphery to the *trans*-Golgi area (bile canalicular region) of the hepatocyte (9). They suggest that pIgA is sorted from asialoglycoproteins in this tubule network, with packaging of pIgA in vesicles for subsequent transport to the bile front. Thus, there is not yet agreement as to the pathway by which pIgA traverses the hepatocyte.

In this study we have extended the findings of Takahashi et al. (37) and Geuze et al. (9). A horseradish peroxidase (HRP) conjugate of mouse ^{125}I-pIgA (^{125}I-pIgA-HRP) and electron microscopic cytochemistry were used to identify and quantitate the intracellular structures involved in the uptake, accumulation, and release of pIgA by rat hepatocytes. We have found that 85% of the total ^{125}I-pIgA-HRP-containing structures at all times analyzed were discrete vesicles, with tubules and multivesicular bodies composing the remaining 15%. In addition, we have found that the vesicles in the bile canalicular region of the hepatocyte tended to be larger than those in the sinusoidal region, which suggests that the ligand is repackaged during transport. Finally, serial sections showed that in most cases vesicles and tubules were not interconnected. Preliminary portions of this work have been presented elsewhere (11).

MATERIALS AND METHODS

Materials

Phosphorylcholine chloride (calcium salt) and *o*-dianisidine dihydrochloride were from Sigma Chemical Co. (St. Louis, MO); complete and incomplete Freund's adjuvant were from Difco Laboratories Inc. (Detroit, MI); and female New Zealand white rabbits (10–12 lb) were supplied by Bunnyville (Littletown, PA). The phosphorylcholine$_{25}$-bovine serum albumin-Sepharose 4B (PC_{25}-BSA-Sepharose 4B) was a generous gift of Dr. Y. C. Lee, Johns Hopkins University. Rabbit anti-rat SC antibody was produced using soluble SC from rat bile as an immunogen. Other reagents were obtained from the same sources given in recent publications from this laboratory (1, 6, 14, 29, 41, 42) or were of the highest purity available commercially and were used without further purification.

Preparation of pIgA

The plasmacytoma cell line, TEPC15, produces an IgA that binds phosphorylcholine (26) and was kindly supplied by Dr. Potter (National Cancer Institute, National Institutes of Health) and Litton Bionetics (Kensington, MD). The cells were grown in the ascites form in pristane-primed BALB/c mice where IgA concentrations reached 4–6 mg/ml ascites. Cells and clotted blood were removed from the ascites by centrifugation (1,300 *g*, 15 min), and sodium azide was added to a final concentration of 3 mM. The ascites could be stored in this state at 4°C for at least 8 mo.

The entire purification of pIgA was done at 4°C. Ascites fluid (25 ml) was clarified by centrifugation (100,000 *g*, 60 min) and then applied to a PC_{25}-BSA-Sepharose 4B affinity column (2 × 5 cm) that had been equilibrated in 0.15 M NaCl, 20 mM Tris-HCl, pH 7.4 (TBS). The column was washed with 10 column vol TBS until absorbance at 280 nm reached 0.04. 5 mM phosphorylcholine chloride in TBS was used to elute IgA in a peak that was 24 ml (1.5 column vol). Monomer and polymer forms of IgA were separated on a Sephadex G-200 column (2.5 × 100 cm), equilibrated, and run in TBS. The fractions were analyzed by native polyacrylamide gel electrophoresis (PAGE), and only those fractions that contained pIgA were pooled. The polymer content of the affinity column IgA pool ranged between 50 and 80% and of the final pIgA after gel filtration between 98 and 100% by densitometric analysis of polyacrylamide gels. The final preparation was >98% IgA as judged by SDS PAGE (in 7.5 and 7–12% polyacrylamide gels) using Coomassie Blue staining and autoradiography of gels of ^{125}I-pIgA. Aliquots were frozen in liquid nitrogen and stored at −70°C.

Preparation and Characterization of pIgA-HRP

pIgA-HRP was prepared according to the procedure of Wall et al. with two modifications (41). Oxidized HRP (1.33 mg) was added to 10 mg ^{125}I-pIgA (4.31×10^4 cpm/μg) for the coupling reaction, and sodium cyanoborohydride (34 mM) was substituted for sodium borohydride in the reduction step. Unconjugated HRP was removed from conjugated and unconjugated ^{125}I-pIgA on a PC_{25}-BSA-Sepharose 4B affinity column (0.8 × 3 cm). The pooled elution peak, which contained both conjugate and free ^{125}I-pIgA, was designated ^{125}I-pIgA-HRP conjugate. The amount of HRP protein in the final conjugate was determined from activity measurements, by comparison with an HRP standard that had been oxidized but not coupled to pIgA. The final conjugate (three preparations) ranged from ~4 to 200 μg HRP bound per 100 mg ^{125}I-pIgA, or 0.005 to 0.4 mol HRP/mol pIgA (using M_r 700,000 for pIgA). The ^{125}I-pIgA-HRP was further characterized by native PAGE and by comparison of its transport kinetics to that of unconjugated ^{125}I-pIgA. ^{125}I-pIgA-HRP was stored at −70°C.

In Vivo Clearance and Transport into Bile

ASSESSMENT OF ^{125}I-pIgA AND ^{125}I-pIgA-HRP CLEARANCE FROM THE BLOOD AND TRANSPORT INTO BILE: The in vivo clearance and transport of ^{125}I-pIgA (1–1,000 μg) and ^{125}I-pIgA-HRP (300–800 μg) were determined as previously described for other liver-specific ligands (12). The bile duct was cannulated with PE-10 Intramedic polyethylene tubing (Clay-Adams, Parsippany, NJ), and bile was collected over 10-min intervals from 0–30 min, 15-min intervals from 30–60 min, and 30-min intervals thereafter.

CHARACTERIZATION OF ^{125}I-pIgA AND ^{125}I-pIgA-HRP IN SERUM AND BILE SAMPLES BY AFFINITY CHROMATOGRAPHY: Serum and bile samples containing ^{125}I-pIgA or ^{125}I-pIgA-HRP were diluted 1/10 in TBS, 0.05% (wt/vol) BSA and applied to a small PC_{25}-BSA-Sepharose 4B column (0.8 × 3.0 cm), and 0.3-ml fractions were collected as described above (Preparation of pIgA) with 0.05% (wt/vol) BSA in all column buffers.

Native PAGE

pIgA samples were analyzed on 5–7% polyacrylamide slab gels according to the method of Maizel (19) as previously described (13), but SDS was omitted from both resolving and stacking gels to prevent dissociation of light chains from the polymers. Samples were applied in 50 mM Tris-HCl, pH 8.9, 0.4 M sucrose, 0.002% (wt/vol) bromphenol blue. Since separation of the pIgA polymers required prolonged electrophoresis, horse spleen ferritin (300 μg) was used as a standard, and the gel was stopped when the fastest running band (M_r of apoferritin, 460,000) had migrated two-thirds the length of the gel. Gels were stained with Coomassie Blue, destained (19), and dried. If ^{125}I-pIgA was being analyzed, the dried gel was exposed to x-ray film (Kodak XAR-5). Bands on the developed film were quantitated using a GS300 Transmittance/Reflectance Densitometer (Hoefer Scientific Instruments, San Francisco, CA) interfaced with a Hewlett-Packard 3390A integrator (Avondale, PA).

Characterization of ^{125}I-pIgA-HRP on Nitrocellulose Transfers

The ^{125}I-pIgA-HRP polymers separated by native PAGE were electrophoretically transferred to nitrocellulose by the method of Towbin et al. (39). The nitrocellulose transfer was quenched with 2% gelatin, 10 mM sodium phosphate, pH 7.4, 0.14 M NaCl, 3 mM KCl before incubation in 1.4 mM 3,3′-diaminobenzidine, 0.03% (wt/vol) H_2O_2, 50 mM Tris-HCl, pH 7.6. Bands of peroxidase reaction product appeared in ~30 s. After two 1-min washes in deionized water, the peroxidase reaction was stopped by the addition of 3% (wt/vol) trichloroacetic acid. After 15 min, the transfer was rinsed in deionized water, blotted dry, and exposed to x-ray film at −70°C with intensifying screen, and the film was developed.

Morphology

LOCALIZATION OF ^{125}I-pIgA-HRP IN SITU: ^{125}I-pIgA-HRP (0.5–1.0 mg pIgA) and mannan (1.0 mg) were mixed and injected into the saphenous vein of fasted Sprague-Dawley rats under phenobarbital anesthesia, and at various times the livers were perfused in situ through the hepatic portal vein, first with 0.9% (wt/vol) NaCl for 10–20 s and then with 2% glutaraldehyde in 0.1 M sodium cacodylate, pH 7.4, for 5 min (12).

HRP activity in the fixed liver was detected as described previously (41). After the diaminobenzidine reaction, sections were rinsed in Tris buffer and treated with 1% OsO_4, 1% $K_4Fe(CN)_6 \cdot 3H_2O$, 0.1 M sodium cacodylate, pH 7.4 (filtered through a Millipore type GS filter, 0.22 μm, Millipore Corp., New Bedford, MA) for 45 min at 4°C (3). After they were rinsed in deionized water at 23°C for 30 s, the sections were dehydrated and embedded in Epon for electron microscopy.

QUANTITATION OF ^{125}I-pIgA-HRP-CONTAINING STRUCTURES IN HEPATOCYTES: The numbers and distributions of intracellular structures containing ^{125}I-pIgA-HRP were determined on thin sections from livers fixed at various times after in vivo injection of ligand. Structures were counted with the aid of a magnifying glass from random micrographs printed at a final magnification of 8,000. The hepatocyte cytoplasm was divided into three regions (sinusoidal, bile canalicular, and intermediate) and the number of ^{125}I-pIgA-HRP-containing structures quantified in each of the regions. A structure was considered to be sinusoidal when found within 1.6 μm of the base of sinusoidal plasma membrane microvilli, bile canalicular when found within 2.2 μm of the base of bile canalicular plasma membrane, and intermediate if a structure did not fall into either of the other two regions.

Golgi-lysosome regions of hepatocytes were defined morphologically as areas in which Golgi stacks and lysosomes could be identified, and in most cases rough endoplasmic reticulum and mitochondria were absent. About 50% of such areas were near bile canaliculi (within ~2.2 μm), and the remainder were in intermediate regions as defined above. ^{125}I-pIgA-HRP-containing vesicles, tubules, and multivesicular bodies were quantified in the Golgi-lysosome regions of the hepatocyte. Vesicles and tubules tended to have a homogeneous intensity of internal HRP reaction product, whereas multivesicular bodies were larger structures in most cases and contained distinguishable internal vesicles or other inclusions. The diameters of ^{125}I-pIgA-HRP-positive vesicles in the sinusoidal, bile canalicular, and intermediate regions were measured on micrographs of cells from livers fixed at 7.5, 15, and 30 min after injection of the conjugate.

ANALYSIS OF ^{125}I-pIgA-HRP-CONTAINING STRUCTURES USING SERIAL SECTIONS: The size, shape, and possible interrelationships of conjugate-containing structures were examined on serial 70-nm sections of tissue from livers fixed 15 and 30 min after ^{125}I-pIgA-HRP injection. Section thickness was calculated as one-half the width of section folds measured on micrographs of known (and calibrated) magnification. 13 series of 6–14 sections each (average of 8/series) were examined.

Other Methods

ACID PRECIPITATION OF ^{125}I-pIgA: Samples of bile, plasma and liver homogenate were incubated at 4°C for 30 min in 10% (wt/vol) trichloroacetic acid, 0.5% (wt/vol) phosphotungstic acid, 1 mM KI, and then sedimented (1,300 *g*, 15 min) at 4°C. The pellet was washed once with the trichloroacetic acid/phosphotungstic acid solution before the radioactivity associated with it was determined. The precipitated radioactivity was a measure of ^{125}I covalently attached to pIgA.

RADIOIODINATION OF PROTEINS: The pIgA was radioiodinated as described previously (14) to 3–5 × 10^9 cpm/mg, stored in aliquots at −70°C, and used within 6 wk after radioiodination. Protein A was radioiodinated by a chloramine-T procedure to a specific activity of 2–4 × 10^{10} cpm/mg (29).

RESULTS

Biochemical Characterization of ^{125}I-pIgA Transport

^{125}I-pIgA CLEARANCE AND TRANSPORT TO BILE: The concentration of ^{125}I-pIgA in blood reached a maximum between 2.5 and 10 min after intravenous injection of the ligand and then decreased steadily out to 180 min (Fig. 1). Radioactivity was first detected in bile 20 min after ligand injection and reached its highest concentration there between 30 and 60 min (Fig. 1). Routinely, by 3 h 30–40% of the injected radioactivity had been transported to bile, a value that was independent of the ^{125}I-pIgA levels administered, which ranged from 1 μg to 1 mg (inset, Fig. 1).

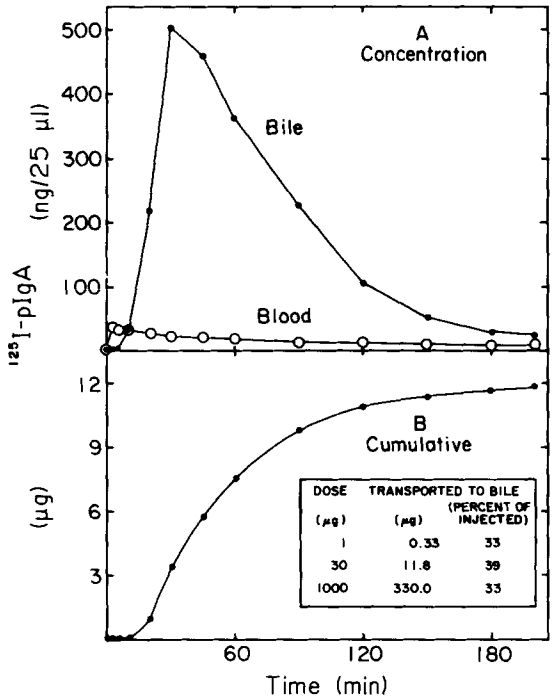

FIGURE 1 The transport of intravenously injected ^{125}I-pIgA into the bile. ^{125}I-pIgA (30 μg) was injected into the saphenous vein of a rat. At various times, the radioactivity present in bile (●) and blood (○) was measured (see Materials and Methods). (*A*) The concentration of ^{125}I-pIgA in bile and blood. (*B*) The cumulative transport of ^{125}I-pIgA into bile. The inset shows the amounts of ^{125}I-pIgA transported into bile after 3 h for three doses of pIgA. This experiment is representative of seven separate experiments.

In seven separate experiments, the distribution of radioactivity 180 min after injection was as follows (mean ± SD): 36 ± 4% was transported to bile, 11 ± 3% was in liver, and 34 ± 7% remained in the blood. An average of 81 ± 9% of the injected radiolabel could be accounted for in bile, blood, and liver, with the remaining 15–20% in the stomach, intestine, thyroid, spleen, kidney, lung, colon, and heart. 180 min after injection of ^{125}I-pIgA, <20% of the radioactivity in liver homogenate and >80% of the radioactivity in stomach and intestine contents were acid soluble. Therefore, ~12% of the injected radioactivity was recovered in a degraded form (iodide or small peptides) from the stomach, intestine, and liver.

CHARACTERIZATION OF ^{125}I-pIgA TRANSPORTED TO BILE: The nature of the radioactivity in the bile was investigated to ascertain that ^{125}I-pIgA was being transported intact across the hepatocyte. More than 90% of the radioactivity collected in bile samples up to 90 min was acid insoluble. Thereafter, the acid-insoluble radioactivity fell but was never less than 70% of the total up to 180 min.

Native PAGE followed by autoradiography was used to compare transported radioactivity with the injected ^{125}I-pIgA (Fig. 2). Three ^{125}I-pIgA bands were present in the injected sample. We have designated the three ^{125}I-bands as the dimer (band 3), tetramer (band 2), and hexamer (band 1) forms of pIgA, based on their elution behavior from the Sephadex G-200 column used to purify pIgA. These assignments are consistent with data on pIgA from three other mouse plas-

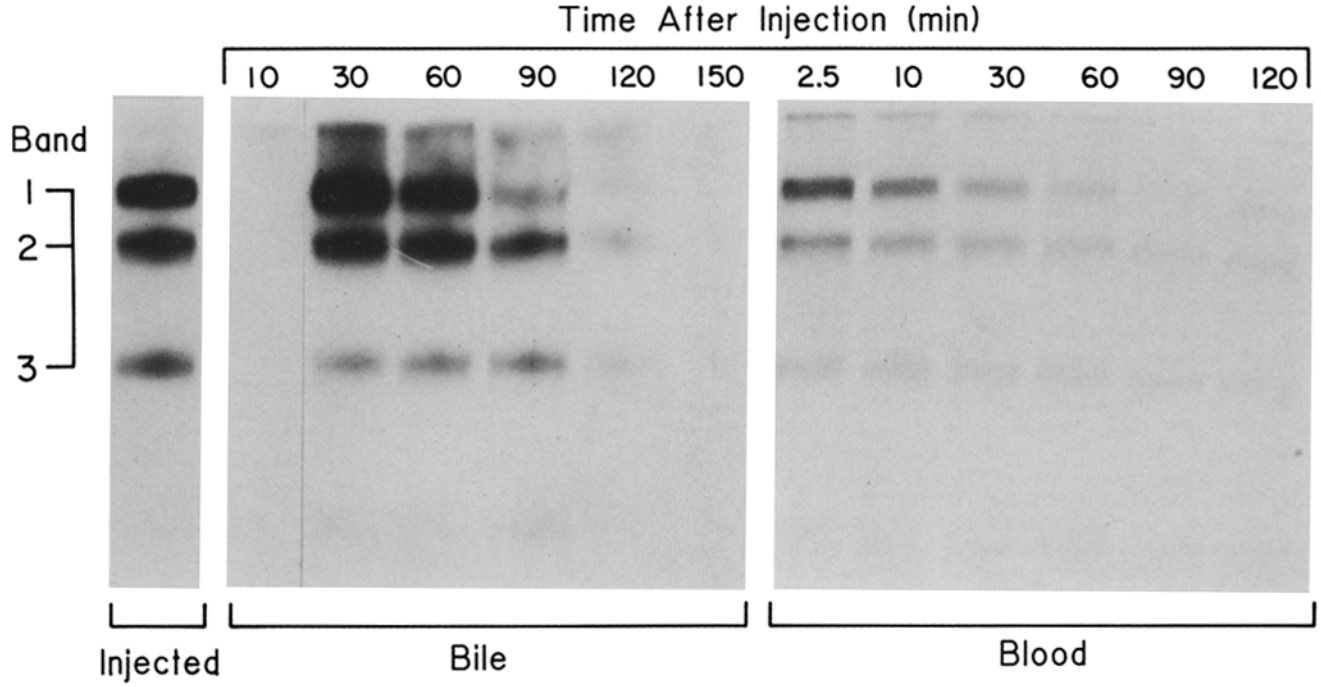

FIGURE 2 Autoradiogram of ^{125}I-pIgA in blood and bile. Bile (25 μl) and plasma (12 μl) samples from the experiment shown in Fig. 1 were analyzed by native PAGE (see Materials and Methods). Bands 3, 2, and 1 represent the polymeric forms of pIgA in our preparation which we believe to be dimer, tetramer, and hexamer, respectively. When this experiment was repeated, the distributions of radioactivity in bands 1–3 of all bile and blood samples were similar to that of the injected material.

macytomas, where tetramer and hexamer accounted for 42–76% (by weight) of the pIgA (10). Bile samples collected at 30, 60, 90, and 120 min had radioactive bands that co-electrophoresed with the three ^{125}I-pIgA bands present in the injected sample. No radiolabeled ligand was detected in bile before 15 min, consistent with the radioactivity measurements. Although the experimental results presented in Fig. 2 suggest that higher polymer forms of pIgA were transported to bile faster than was the dimer, the experiment was repeated using a new pIgA preparation, and no apparent rate differences were observed. Thus, it is not at present clear to what extent the various polymeric species produced by the mouse TEPC plasmacytoma are differentially transported from blood to bile. However, when rat bile from uninjected animals was analyzed by native PAGE and immunoblotting (14) with an anti-alpha chain antibody, endogenous dimer, tetramer, and hexamers of IgA were all present, which indicates that the rat system can transport these polymers, whether endogenous or exogenous in origin.

^{125}I-pIgA collected in bile samples up to 90 min, and the injected ^{125}I-pIgA showed the same extent of binding and specific hapten elution from PC_{25}-BSA-Sepharose 4B columns, which was 70–80% of that applied. This indicated that the intact ^{125}I-pIgA in bile was immunologically active after its transport across the hepatocyte and secretion. The immunoprecipitation of SC (using rabbit anti-SC) from bile samples collected 30–60 min after ^{125}I-pIgA injection indicated that at least 40% of the transported ^{125}I-pIgA was bound to SC (data not shown).

CHARACTERIZATION OF CIRCULATING ^{125}I-pIgA: More than 80% of the radioactivity in all plasma samples collected from 0–180 min was acid precipitable, and results of native PAGE revealed the presence of three ^{125}I-pIgA bands that co-electrophoresed with those present in injected ^{125}I-pIgA samples (Fig. 2). Since by these criteria the ^{125}I-pIgA remaining in the circulation at 120 min was intact, it was puzzling why all of the molecules initially injected were not cleared. Comparable amounts (70–80%) of ligand from both injected and 120-min plasma samples bound to and were specifically eluted from PC_{25}-BSA-Sepharose columns, which indicates that antigen binding was retained in the uncleared pIgA. To examine the possibility that liver transport was progressively impaired during the experiment, a rat that had been injected 2 h earlier with a dose of ^{125}I-pIgA was challenged with another dose of ^{125}I-pIgA at 10 times greater specific activity. The result was unequivocal. The second ^{125}I-pIgA dose was transported into bile with kinetics identical to that of the first. Another possibility, that the ^{125}I-pIgA remaining in the plasma at 120 min could not be cleared, was addressed by a study of its behavior after administration to a second rat. Serum prepared from the blood of a rat that had been injected 2 h earlier with high specific activity ^{125}I-pIgA was injected into a second rat. Calculated on the basis of the ^{125}I-pIgA dose given to the first rat, only 4% more was cleared in the second animal, which indicates the near-complete inability of this ^{125}I-pIgA to be transported into the bile. We concluded that either a population of ^{125}I-pIgA less active in transport was produced after injection into rats, or ^{125}I-pIgA existed as a heterogeneous population of molecules before injection.

Assessment of ^{125}I-pIgA-HRP Conjugate

We next determined the clearance and transport characteristics of the HRP conjugate of ^{125}I-pIgA. The low endogenous HRP activity in bile allowed a direct comparison of the radioactivity and peroxidase activity transported to bile in our initial characterization of the conjugate. The kinetics of ^{125}I-pIgA-HRP transport into bile measured both ways was similar

to that of ^{125}I-pIgA (Figs. 1 and 3). Both radioactivity and peroxidase activity first appeared in bile at 20 min and reached a maximum concentration at 60 min, within the 30–60-min period in which bile ^{125}I-pIgA usually reached a maximum. However, more of the injected peroxidase activity (56%) than of the injected radioactivity (38%) was transported to bile (inset, Fig. 3). The ^{125}I-pIgA-HRP radioactivity present in the liver (23% of injected) after the 120-min experiment was somewhat higher than the 6–15% range seen for the 180-min experiments. This probably reflects the greater percentage of injected ^{125}I-pIgA-HRP in transit through the hepatocyte at 120 min.

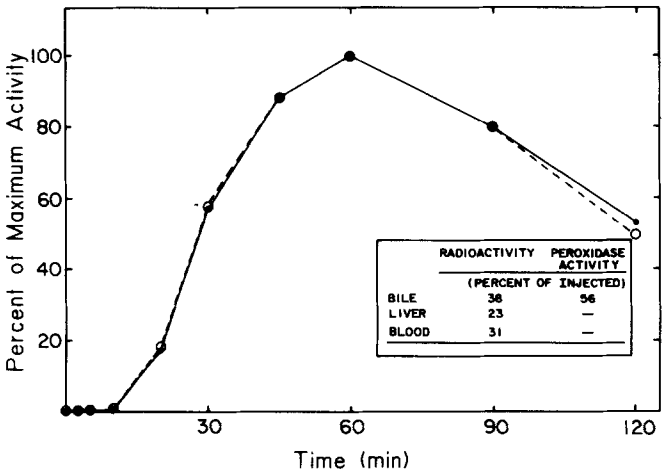

FIGURE 3 The transport of intravenously injected ^{125}I-pIgA-HRP conjugate into the bile. ^{125}I-pIgA-HRP (300 μg pIgA) was injected into the saphenous vein of a rat, and at various times the radioactivity (○) and peroxidase activity (●) in bile were determined. The inset shows the distribution of 92% of the radioactivity and a comparison of the radioactivity and peroxidase activity in the bile at 120 min. Peroxidase activity of the conjugate could not be determined in liver and blood due to high endogenous activity.

We next characterized the injected and transported conjugates by native PAGE, the results of which are shown in Fig. 4. The three bands observed with ^{125}I-pIgA alone were also present in the injected preparation of ^{125}I-pIgA-HRP and contained both radiolabel and HRP activity. A comparison of the relative amounts of radioactivity and peroxidase activity in each band indicated that HRP was preferentially coupled to higher polymeric forms. There was also radioactivity at the top of the separating gel that had relatively less HRP activity (Fig. 4, *A* vs. *B*). This radiolabeled material may represent species that have more than one pIgA molecule bound per HRP molecule, with possible inactivation of HRP in such conjugates. When the ^{125}I-pIgA-HRP transported to bile was analyzed on native gels, both radioactivity and HRP activity were detected in the three pIgA bands that corresponded to the major pIgA's injected (Fig. 4). A discrete band containing HRP activity was also present above band 1, but its content of ^{125}I was not detectable above the background in that region of the gel (Fig. 4*B*).

Finally, we found that >70% of both peroxidase activity and radioactivity transported to bile between 45 and 60 min after ^{125}I-pIgA-HRP injection was bound and specifically eluted from PC_{25}-BSA-Sepharose 4B. Thus, by several criteria, the HRP in bile was coupled to ^{125}I-pIgA, which indicates that the conjugate had crossed the hepatocyte intact.

Ultrastructural Examination of ^{125}I-pIgA-HRP Transport Across the Hepatocyte

To characterize the transport of ^{125}I-pIgA-HRP across the hepatocyte, the types and cellular distribution of structures that contained this electron microscopic tracer were determined at various times after in vivo administration of the conjugate. Fig. 5 illustrates qualitatively the types of ^{125}I-pIgA-HRP-containing structures present in the sinusoidal, intermediate, and bile canalicular regions of hepatocytes 30 min

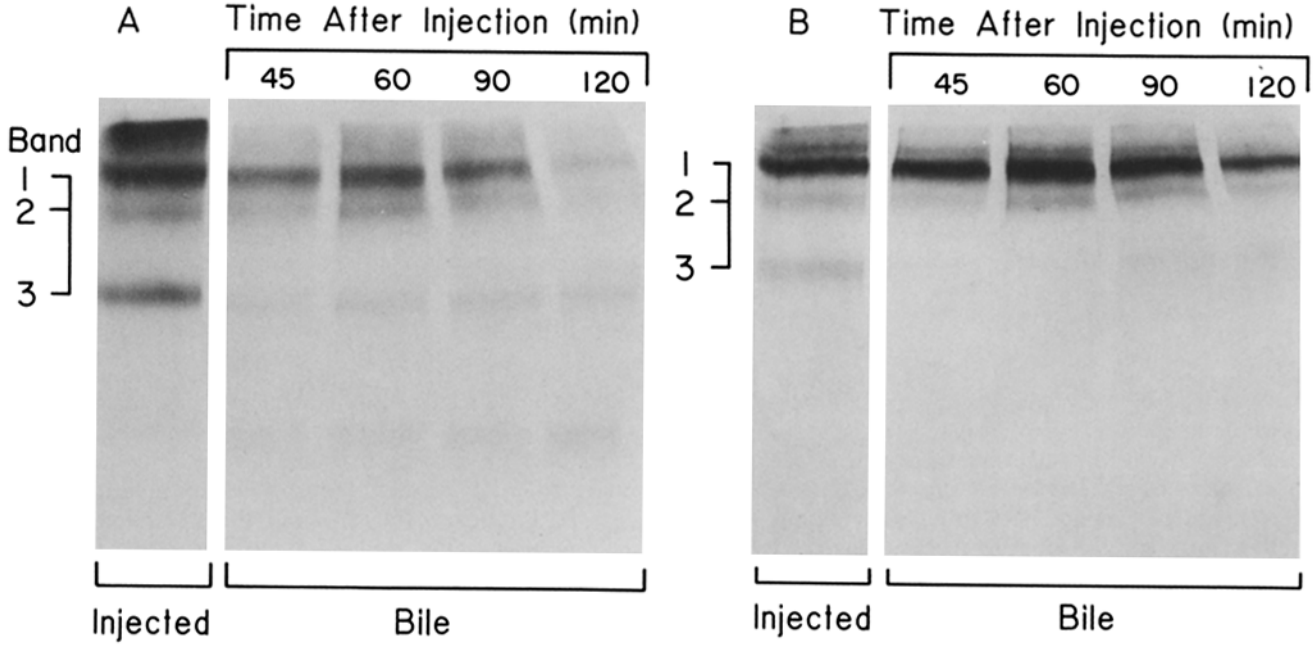

FIGURE 4 Analysis of the radioactivity and peroxidase activity of the ^{125}I-pIgA-HRP transported to bile. Bile samples were separated by native PAGE and then electrophoretically transferred to nitrocellulose. The transfer was analyzed for HRP activity and radioactivity as described in Materials and Methods. (*A*) Autoradiogram. (*B*) Peroxidase activity.

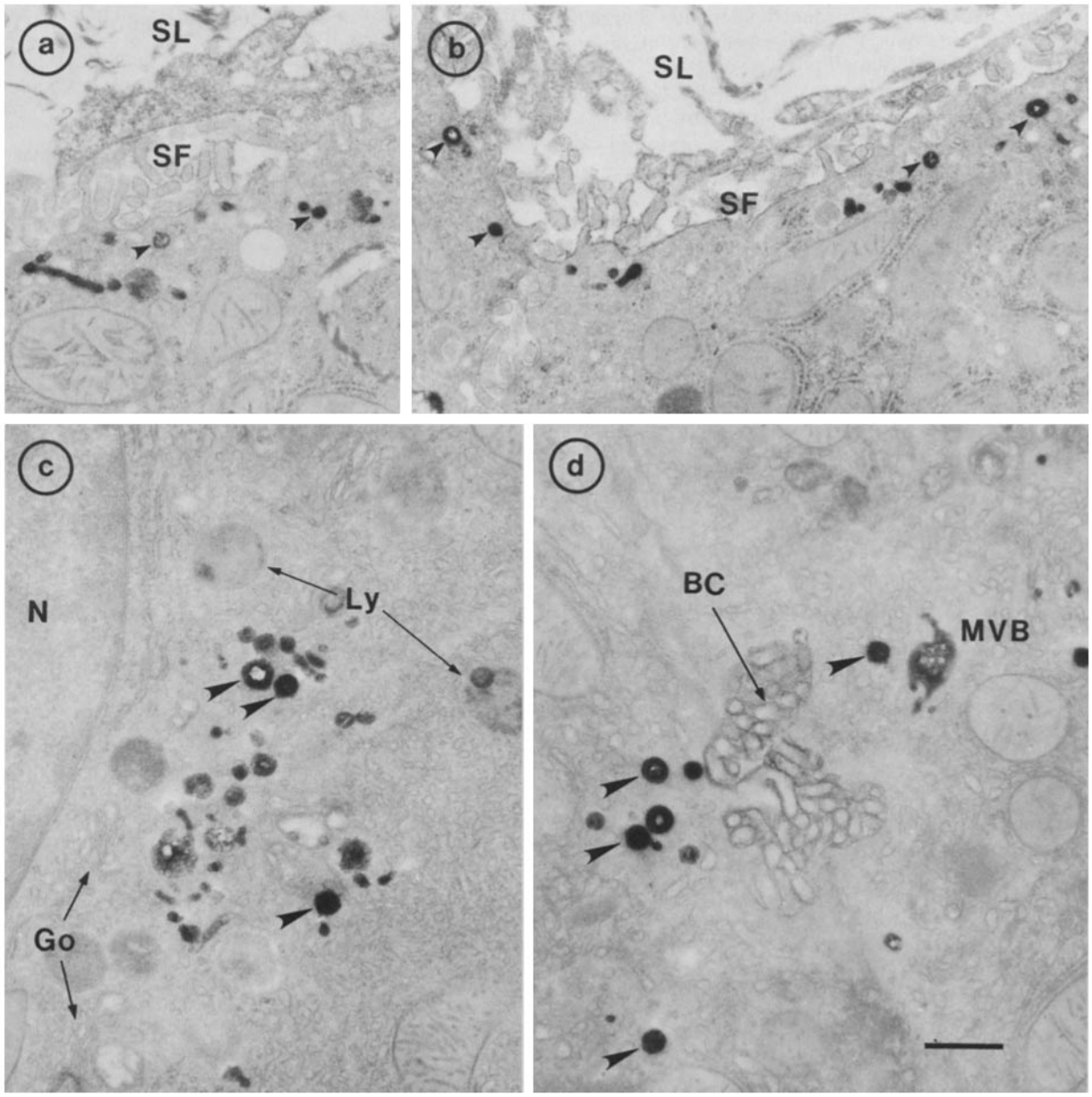

FIGURE 5 Intracellular localization of pIgA-HRP in hepatocytes after its in vivo administration. Livers were fixed by perfusion 30 min after in vivo injection of the conjugate (0.55 mg) and processed for HRP cytochemistry. (*a* and *b*) Sinusoidal region. HRP reaction product is present in small vesicles (small arrowheads) and tubules. *SL*, sinusoidal lumen; *SF*, sinusoidal front. (*c*) Intermediate region. Reaction product is found near nuclei (*N*), and in vesicles similar in size to those at the periphery, in multivesicular bodies, and also in larger vesicles (large arrowheads), but not in lysosomes (*Ly*) or stacks of Golgi (*Go*), which are also in this area. (*d*) Bile canalicular (*BC*) region. Conjugate is present in larger vesicles (large arrowheads) and in multivesicular bodies (*MVB*) as well as in the bile canaliculus itself. Bar, 0.5 μm. × 24,000.

after injection of the conjugate, when the distribution of labeled structures was approximately equal in these regions. Vesicles were the predominant labeled structures seen in every region of the cell at all times after injection. They accounted for ~85% of all ^{125}I-pIgA-HRP-structures, with tubules and multivesicular bodies composing the rest. However, the sizes of labeled vesicles found in the sinusoidal region (Fig. 5, *a* and *b*) tended to be smaller than those near the bile canaliculus (Fig. 5*d*). Our quantitation of these qualitative observations is presented below.

CELLULAR DISTRIBUTION OF ^{125}I-pIgA-HRP-CONTAINING STRUCTURES: To obtain an indication of the pathway and kinetics of ligand transport, the cellular distribution of ^{125}I-pIgA-HRP structures was determined at various times after intravenous injection of conjugate. The results presented in Table I show a progressive redistribution of ^{125}I-pIgA-HRP structures from the sinusoidal area to intermediate and bile canalicular regions of the hepatocyte cytoplasm between 2.5 and 10 min after administration of ^{125}I-pIgA-HRP. The percentage of structures in the sinusoidal region decreased from 94 to 47 in this period, approaching a steady state at ~40% of total structures. The conjugate appeared in structures in the intermediate region before the bile canalicular region, which suggests that ^{125}I-pIgA-HRP was delivered

to the intermediate region immediately after the sinusoidal region (see 2.5 min in Table I). The percentage of structures in the intermediate region reached a maximum at 10–12.5 min (at 34 and 36%, respectively) and decreased steadily thereafter. The rate at which the percentage of total structures in the bile canalicular region increased for the first 15 min (from 0 to 30%) was faster than the increase between 15 and 45 min (from 30 to 39%). As illustrated qualitatively in Fig. 5, most labeled structures were vesicles. When the diameters of ^{125}I-pIgA-HRP vesicles in the three cellular regions of livers fixed 7.5, 15, and 30 min after conjugate injection were measured, vesicles in the bile canalicular region were found to be larger than those in the sinusoidal area of the hepatocyte. The results are presented in Fig. 6. The sizes of vesicles in the intermediate compartment fell between those in the other two regions (data not shown).

^{125}I-PIGA-HRP STRUCTURES IN THE GOLGI-LYSOSOME AREA: Previous work from this laboratory established that epidermal growth factor (6) and asialoglycoproteins

TABLE I. *Distribution of pIgA-HRP-containing Structures in Hepatocytes After In Vivo Injection*

Time after administration (*min*) (total structures counted)	Conjugate preparation used	Intracellular region (% of total structures)		
		Sinusoidal*	Intermediate	Bile canalicular‡
2.5 (65)	3	94	6	0
5 (351)	2, 3, 4	86	10	4
7.5 (570)	4	57	24	19
10 (1,038)	3, 4	47	34	19
12.5 (553)	4	37	36	27
15 (1,338)	2, 3, 4	45	25	30
30 (1,286)	3	35	29	36
45 (125)	3	40	21	39

Livers were fixed in situ at various times after administration of ^{125}I-pIgA-HRP (0.5–1.0 mg pIgA) and mannan (1.0 mg) and then processed for peroxidase cytochemistry as described in Materials and Methods. Each discrete structure was scored as one, regardless of size and shape. Since three separate preparations of conjugate have been used in the above experiments, the conjugate(s) used for each administration time is indicated. The standard deviation was <10% for the combined data at 5 and 10 min and in the intermediate region at 15 min. However, the combined data for the sinusoidal and bile canalicular regions at 15 min had standard deviations of 18 and 16%, respectively. The data for each region are presented as a percentage of total structures scored at a given time.

* Structures within 1.6 μm of the base of the sinusoidal plasma membrane microvilli.

‡ Structures within 2.2 μg of the base of the bile canalicular plasma membrane.

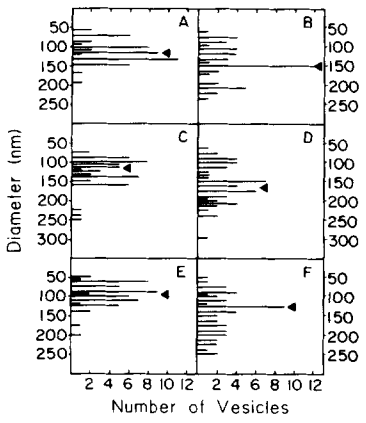

FIGURE 6 The distribution of vesicle sizes in the sinusoidal and bile canalicular regions. The diameters of ^{125}I-pIgA-HRP-positive vesicles in the sinusoidal (*A*, *C*, and *E*) and bile canalicular (*B*, *D*, and *F*) regions were measured on micrographs of cells from livers fixed at 7.5 (*A* and *B*), 15 (*C* and *D*), and 30 (*E* and *F*) min after injection of the conjugate. 50 vesicles were measured at each time point. Medians are indicated by the arrowheads.

TABLE II. *Classification of pIgA-HRP-containing Structures in Golgi-Lysosomal Regions*

Time after administration	Structures in Golgi-Lysosome region (% of total structures in cell)	Golgi-lysosome region (% of total structures)		
		Tubules*	Vesicles‡	Multivesicular bodies§
min				
2.5	0	—‖	—	—
5	7	0	62	38
7.5	19	4	83	13
10	29	5	80	15
12.5	35	4	75	21
15	31	9	79	12
30	21	8	87	5
45	26	12	78	10

The experiment was the same as that described in Table I. Examples of vesicles, tubules, and multivesicular bodies are shown in the micrographs of Fig. 5.

* Tubular structures ≤700 nm long.

‡ Circular structures ≤295 nm in diameter.

§ Multivesicular bodies are vesicles >200 nm in diameter that contain distinguishable vesicles or other inclusions in their lumen.

‖ No structures in Golgi-lysosomal region of cell.

(41), two ligands destined for lysosomal degradation, accumulated in endosomal structures within the Golgi-lysosome regions of hepatocytes before their entry into bona fide lysosomes. Therefore, we identified and quantified the ^{125}I-pIgA-HRP-containing structures in such regions to determine if a similar accumulation was occurring before secretion of pIgA (Table II). Ligand did enter Golgi-lysosome regions early and reached significant proportions there (~30% of total structures) before biochemical evidence of release into bile (>15 min). However, approximately half of these regions were very near bile canaliculi (~2.2 μm). More important, most labeled structures were neither stacks of Golgi complexes, lysosomes, nor endosomes typical of those in which lysosomal ligands accumulate. Rather, pIgA-HRP was found predominantly in vesicles, as it was in all other regions of the cell. However, the combined percentage of tubules and multivesicular bodies in Golgi-lysosome areas was somewhat greater than that found over all cellular regions (~13–25 vs. 15%). Nonetheless, there was remarkably little change in the distribution of ^{125}I-pIgA-HRP among vesicles, tubules, and multivesicular bodies in Golgi-lysosomal areas for times after 5 min.

ELECTRON MICROSCOPIC SERIAL SECTION ANALYSIS OF ^{125}I-PIGA-HRP-CONTAINING STRUCTURES: Many sets of serial sections were examined to obtain a clearer picture of the size, shape, and interrelationships of the structures containing ^{125}I-pIgA-HRP. A representative series of nine sections is presented in Fig. 7. Structures identified as vesicles on single micrographs were confirmed to be simple spherical structures in serial sections and between 50 and 295 nm in diameter. Measurements of tubules that were sectioned along their long axis indicated that they could reach at least 700 nm in length. More important, our serial section analysis indicated that the number of tubules was underestimated by only ~5–10%[2] in the analysis of single micrographs presented in

[2] The analysis in Table II underestimated the number of tubules by only 5–10%. This estimate was obtained by counting conjugate-containing structures in a single micrograph from a serial section sequence and then carefully examining the remaining micrographs to determine the percentage of tubules counted as vesicles.

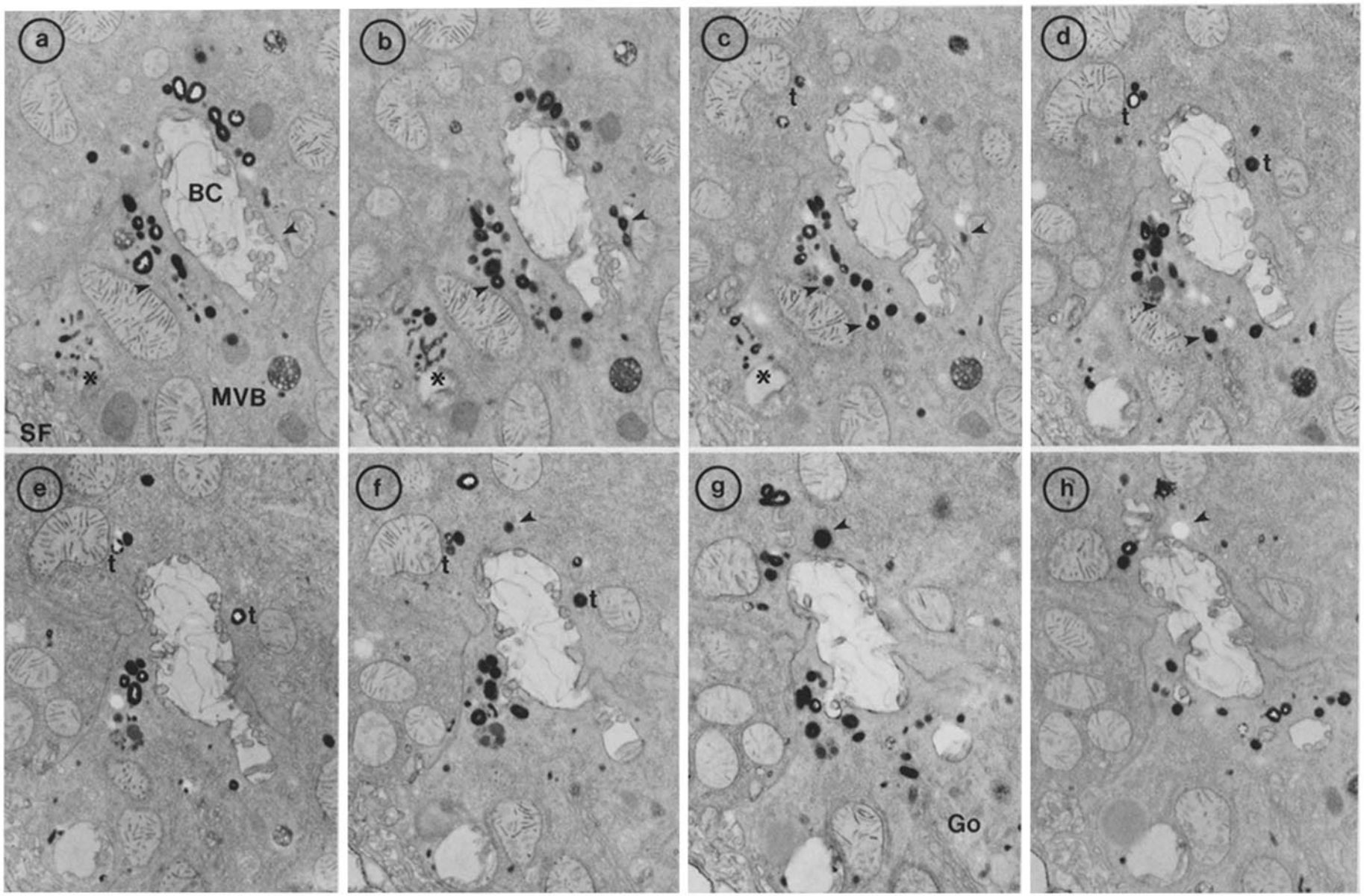

FIGURE 7 Serial section micrographs of bile canalicular and sinusoidal regions in a liver 30 min after pIgA-HRP administration. Livers were fixed by perfusion and processed for HRP cytochemistry. The predominant labeled structures around the bile canaliculus (*BC*) are discrete vesicles that span a maximum of three 70-nm sections. Several are marked by small arrowheads. Tubules (*t*) span more than three successive sections, and multivesicular bodies (*MVB*) span more than five. Near the sinusoidal front (*SF*), reaction product is in an anastomosing network of tubules and several small vesicles (* in *a–c*). *Go*, Golgi complex. × 16,000.

Table II (due to tubules sectioned transverse to their long axis, or close to transverse, appearing as vesicles as in Fig. 7, *c–f*). Multivesicular bodies (*MVB* in Fig. 7, *a–e*) were large, somewhat spherical structures >200 nm in diameter. These structures were occasionally seen in continuity with tubules (see Fig. 5), and in some cases vesicles appeared to be in continuity with tubules (e.g., see Fig. 7, *b* and *c*).

DISCUSSION

The purpose of this study was to characterize the transcellular transport of pIgA across the rat hepatocyte. Toward this goal, we biochemically characterized the transport of our ^{125}I-pIgA (TEPC15) and electron microscopic tracer (^{125}I-pIgA-HRP). Once satisfied that these molecules were being transported as expected, we undertook electron microscopic studies to characterize the pIgA transport pathway.

Biochemical Characterization of ^{125}I-pIgA and pIgA-HRP Transport

Unlike asialoglycoproteins and asialo,agalactoglycoproteins, where >80% of the injected dose is cleared by the liver in 10 min (12), ^{125}I-pIgA is cleared both less effectively and more slowly (40–55% in 180 min). The results indicate that mouse ^{125}I-pIgA may exist as a mixture of transport-active and -inactive molecules before injection into animals. Perhaps SC-binding sites on some of the pIgA molecules are inactivated during the preparation of pIgA or its radioiodination. Alternatively, the transport-inactive molecules may lack their J chain and be unable to bind to their receptor, as Brandtzaeg and Prydz have suggested (2). However, values in the literature for rat and human ^{125}I-pIgA uptake by the rat agree nicely with ours and are from 30 to 67% of injected ^{125}I-pIgA transported to bile in intact rats (17, 22, 25, 30, 40), 27% in an isolated perfused liver (7), and 53% in cultured hepatocytes (18).

When we analyzed the specific electron microscopic tracer, ^{125}I-pIgA-HRP, we found that the transport kinetics of both radioactivity and peroxidase activity were similar (Fig. 3); however, relatively more peroxidase activity was transported to bile than was radioactivity. This difference may have been caused by the nature of the pIgA to which HRP was conjugated. HRP was reacted with a mixture of pIgA that contained one part ^{125}I-pIgA and 100 parts unlabeled pIgA. Therefore, HRP was coupled mainly to unlabeled pIgA. The greater transport of HRP activity could therefore be accounted for by better binding of the unlabeled pIgA-HRP conjugate to SC than to the labeled pIgA and labeled conjugate. Thus, the pIgA-HRP conjugate is probably a better probe of pIgA transport than is the radioiodinated ligand. The substantial transport of both pIgA and peroxidase activity (Fig. 3), together with our finding that ^{125}I-pIgA-HRP was transported into bile as an intact conjugate, indicated that the localization of HRP-containing structures accurately reflected the behavior of pIgA itself.

Electron Microscopic Study of ^{125}I-pIgA-HRP Transport

The distribution of ^{125}I-pIgA-HRP-containing structures in the hepatocyte during the continuous uptake of conjugate indicated that after internalization at the sinusoidal front, ^{125}I-pIgA-HRP rapidly appeared in both the intermediate and bile canalicular regions of cells (Table I). ^{125}I-pIgA-HRP-containing structures could be detected in the latter region as early as 5 min after administration of the conjugate, and their percentage continued to increase up to 45 min. Within the intermediate and bile canalicular regions, many of the labeled structures could be localized to areas in which Golgi complexes and lysosomes were also present. HRP conjugates of asialoorosomucoid (41) and epidermal growth factor (6), two polypeptides destined for lysosomal degradation, appear in Golgi-lysosome areas of hepatocytes 4–5 min after their administration, the same time at which ^{125}I-pIgA-HRP structures appeared in these areas (Table II). However, the types of structures that contain these conjugates were qualitatively different from those that contain pIgA-HRP. Although none of the three ligands was present in either bona fide stacks of Golgi complexes or in lysosomes, asialoorosomucoid and epidermal growth factors were present in a more complicated array of tubulovesicular structures than those seen for ^{125}I-pIgA-HRP. pIgA was found predominantly in vesicles. The different distributions of lysosome- vs. bile-destined ligands suggest either that these ligands enter the hepatocyte by internalization into different structures or that sorting of these ligands may begin soon after endocytosis and continue to near completion during transit of the molecules to Golgi-lysosomal areas. Alternatively, segregation may occur rapidly in the Golgi-lysosomal areas, with the resulting prelysosomal and presecretion compartments having relatively long residence times. Since HRP conjugates of asialoorosomucoid, epidermal growth factor, and pIgA occur in similar structures in the sinusoidal region of the hepatocyte, we believe they enter cells in the same vesicles and tubules. This would require a sorting of ligands within the cell. The dual ligand experiments of Courtoy et al. and of Geuze et al. support this hypothesis (5, 9).

Several studies have suggested that pIgA is present only in vesicles during its transport across the hepatocyte (4, 21, 37), and another study has implicated smooth endoplasmic reticulum in addition to vesicles in ^{125}I-pIgA transport (27). We saw no evidence for the involvement of smooth endoplasmic reticulum in serial sections of ^{125}I-pIgA-HRP-containing structures (Fig. 7). However, 85% of the total ^{125}I-pIgA-HRP-containing structures were vesicles. Nonetheless, we did find tubules and multivesicular bodies that contained conjugate (Fig. 5). Since vesicles appeared much more often than did tubules or multivesicular bodies in juxtaposition to the bile canalicular plasma membrane, vesicles are probably the structures responsible for secretion of ^{125}I-pIgA into the bile. Furthermore, they were generally larger than ligand-containing vesicles near the sinusoidal front, implying transfer of ligand during its transport, fusion of vesicular carriers, or both. Similar types of large vesicles around bile canaliculi were reported by Renston et al. to contain unconjugated HRP, a fluid-phase pinocytic marker (28). However, this tracer, which was administered at very high doses (10 mg/100 g body wt), was even more abundant in multivesicular bodies and secondary lysosomes of hepatocytes, which suggests that it nonselectively filled all those endocytic pathways that originate at the sinusoidal front (i.e., lysosomal, transcellular, and perhaps as yet unidentified routes). Our ^{125}I-pIgA-HRP conjugate exhibited must greater selectivity and at lower doses.

It is not currently clear why ^{125}I-pIgA-HRP was found in

multivesicular bodies, structures commonly thought to be lysosomal precursors (6, 8, 41). At this time, we cannot exclude the possibility that multivesicular bodies have a role in pIgA transport. We believe a more likely explanation is that some ^{125}I-pIgA-HRP molecules were directed to lysosomes because of simple missorting, or because of an alteration of injected conjugate that still allowed its specific uptake into hepatocytes but not its secretion into bile.

The ^{125}I-pIgA-HRP-containing tubules we have described may be analogous to the compartment of uncoupling of receptors and ligand described by Geuze et al., who used immunoelectron microscopy to detect endogenous pIgA (9). The authors describe this compartment as an interconnected tubule network extending from the sinusoidal cell periphery to the *trans*-Golgi area, with the tubules participating most significantly in pIgA sorting occurring at the sinusoidal-lateral cell corners of the hepatocyte. Our data showed the presence of ^{125}I-pIgA-HRP-containing tubules in both sinusoidal and bile canalicular regions of the cell with no overwhelming preference for one location over the other. In addition, our serial section analysis of ^{125}I-pIgA-HRP-containing structures strongly indicated no interconnections of tubules between the sinusoidal and bile canalicular regions (Fig. 7). Thus, tubules probably do play a role in the transport of pIgA across the hepatocyte, since they are found throughout the hepatocyte, but they appear to be concentrated in the sinusoidal and bile canalicular regions. However, more work is required to resolve the apparent differences between our results and those of Geuze et al. (9), since different morphologic methods were used in the two studies.

^{125}I-pIgA-HRP did not appear in the bile until 20 min, even though significant numbers of ligand-containing structures had accumulated in the bile canalicular region by 10 min (Fig. 3 and Table I). This observation suggested that there was a lag between ^{125}I-pIgA vesicle accumulation in the bile canalicular region and fusion with the bile canalicular plasma membrane. The reason for such a lag is at present unclear but may involve the proteolytic cleavage of the membrane SC (M_r 120,000 in reducing SDS PAGE) to free SC, a step necessary for release of secretory IgA into the bile, since only free SC is detected in bile (34–36).

In conclusion, the quantitative biochemical and morphological approach we used to trace the pathway of pIgA across rat hepatocytes has significantly extended several recent morphological studies on pIgA transport (9, 37). We have shown that relatively simple tubules are involved in ^{125}I-pIgA-HRP transport but that vesicles are the overwhelming intracellular structures containing pIgA. We feel that sorting of pIgA from lysosome-bound ligands either may begin soon after internalization and continue to completion during cellular transport, or may occur rapidly in the Golgi-lysosomal areas of the hepatocyte. The larger size of vesicles in the bile canalicular region of the hepatocyte relative to those in the sinusoidal region suggests that conjugate undergoes some change in "packaging" during its transport across the hepatocyte. Finally, our serial section analysis indicates that there are no extensive interconnections between structures in the sinusoidal and bile canalicular regions, leading us to conclude that pIgA is transported from blood to bile within membrane bound compartments, which themselves move across the hepatocyte, and not through a tubular complex, which connects sinusoidal and bile canalicular regions.

We thank Dr. Michael Potter (National Cancer Institute) and Litton Bionetics (Kensington, MD) for supplying the TEPC15 plasmacytoma cell line, Dr. Y. C. Lee and Nancy Stultz (Johns Hopkins University) for the phosphorylcholine$_{25}$-BSA preparation, Ed Shapland for his technical help, Tom Urquhart for photography of the figures, members of the Hubbard lab for critically reading the manuscript, and Arlene Daniel for preparation of the manuscript.

This work was supported by National Institutes of Health (NIH) grant to Dr. Hubbard (GM29133) and an NIH postdoctoral fellowship to Dr. Hoppe (AM07254).

Received for publication 16 May 1985, and in revised form 16 August 1985.

REFERENCES

1. Bartles, J. R., L. T. Braiterman, and A. L. Hubbard. 1985. Endogenous and exogenous domain markers of the rat hepatocyte plasma membrane. *J. Cell Biol.* 100:1126–1138.
2. Brandtzaeg, P., and H. Prydz. 1984. Direct evidence for an integrated function of J chain and secretory component in epithelial transport of immunoglobulins. *Nature (Lond.).* 311:71–73.
3. Brown, W. J., and M. G. Farquhar. 1984. The mannose-6-phosphate receptor for lysosomal enzymes is concentrated in cis Golgi cisternae. *Cell.* 36:295–307.
4. Courtoy, P. J., J. N. Limet, J. Quintart, Y.-J. Schneider, J. P. Vaerman, and P. Baudhuin. 1983. Transfer of IgA into rat bile: ultrastructural demonstration. *Ann. NY Acad. Sci.* 409:799–802.
5. Courtoy, P. J., J. Quintart, J. N. Limet, C. DeRoe, and P. Baudhuin. 1982. Intracellular sorting of galactosylated proteins and polymeric IgA in rat hepatocytes. *J. Cell Biol.* 95(5, Pt. 2):425a. (Abstr.)
6. Dunn, W. A., and A. L. Hubbard. 1984. Receptor-mediated endocytosis of epidermal growth factor by hepatocytes in the perfused rat liver: ligand and receptor dynamics. *J. Cell Biol.* 98:2148–2159.
6a. Dunn, W. A., T. P. Connolly, and A. L. Hubbard. 1986. Receptor-mediated endocytosis of epidermal growth factor by rat hepatocytes: receptor pathway. *J. Cell Biol.* In press.
7. Fisher, M. M., B. Nagy, H. Bazin, and B. J. Underdown. 1979. Biliary transport of IgA: role of secretory component. *Proc. Natl. Acad. Sci. USA.* 76:2008–2012.
8. Geuze, H. J., J. W. Slot, G. J. A. M. Strous, H. F. Lodish, and A. L. Schwartz. 1983. Intracellular site of asialoglycoprotein receptor-ligand uncoupling: double-label immunoelectron microscopy during receptor-mediated endocytosis. *Cell.* 32:277–287.
9. Geuze, H. J., J. W. Slot, G. J. A. M. Strous, J. Peppard, K. von Figura, A. Hasilik, and A. L. Schwartz. 1984. Intracellular receptor sorting during endocytosis: comparative immunoelectron microscopy of multiple receptors in rat liver. *Cell.* 37:195–204.
10. Halpern, M. S., and R. L. Coffman. 1972. Polymer formation and J chain synthesis in mouse plasmacytomas. *J. Immunol.* 109:674–680.
11. Hoppe, C. A., and A. L. Hubbard. 1984. Transcellular transport of polymeric IgA in the rat hepatocyte. *J. Cell Biol.* 99(4, Pt. 2):282a. (Abstr.)
12. Hubbard, A. L., G. Wilson, G. Ashwell, and H. Stukenbrok. 1979. An electron microscope autoradiographic study of the carbohydrate recognition systems in rat liver. I. Distribution of ^{125}I-ligands among the liver cell types. *J. Cell Biol.* 83:47–64.
13. Hubbard, A. L., and A. Ma. 1983. Isolation of rat hepatocyte plasma membranes. II. Identification of membrane-associated cytoskeletal proteins. *J. Cell Biol.* 96:230–239.
14. Hubbard, A L., J. R. Bartles, and L. T. Braiterman. 1985. Identification of rat hepatocyte plasma membrane proteins using monoclonal antibodies. *J. Cell Biol.* 100:1115–1125.
15. Kleinman, R. E., P. R. Harmatz, and W. A. Walker. 1982. The liver: an integral part of the enteric mucosal immune sytem. *Hepatology.* 2:379–384.
16. Lemaitre-Coelho, I., G. D. F. Jackson, and J.-P. Vaerman. 1977. Rat bile as a convenient source of secretory IgA and free secretory component. *Eur. J. Immunol.* 8:588–590.
17. Lemaitre-Coelho, I., G. Acosta Altamirano, C. Barranco-Acosta, R. Meykens, and J.-P. Vaerman. 1981. *In vivo* experiments involving secretory component in the rat hepatic transfer of polymeric IgA from blood into bile. *Immunology.* 43:261–270.
18. Limet, J. N., Y.-J. Schneider, J. P. Vaerman, and A. Trouet. 1980. Interaction of rat IgA with cultured rat hepatocytes: binding site, drug effects. *Toxicology.* 18:187–194.
19. Maizel, J. V., Jr. 1971. Polyacrylamide gel electrophoresis of viral proteins. *Methods Virol.* 5:179–246.
20. Mostov, K. E., and G. Blobel. 1982. A transmembrane precursor of secretory component. The receptor for transcellular transport of polymeric immunoglobulins. *J. Biol. Chem.* 257:11816–11821.
21. Mullock, B. M., J. P. Luzio, and R. H. Hinton. 1983. Preparation of a low-density species of endocytic vesicle containing immunoglobulin A. *Biochem. J.* 214:823–827.
22. Orlans, E., J. Peppard, J. Reynolds, and J. Hall. 1978. Rapid active transport of immunoglobulin A from blood to bile. *J. Exp. Med.* 147:588–592.
23. Orlans, E., J. Peppard, J. F. Fry, R. H. Hinton, and B. M. Mullock. 1979. Secretory component as the receptor for polymeric IgA on rat hepatocytes. *J. Exp. Med.* 150:1577–1581.
24. Orlans, E., J. V. Peppard, A. W. R. Payne, B. M. Fitzharris, B. M. Mullock, R. H. Hinton, and J. G. Hall. 1983. Comparative aspects of the hepatobiliary transport of IgA. *Ann. NY Acad. Sci.* 409:411–427.
25. Peppard, J., E. Orlans, A. W. R. Payne, and E. Andrew. 1981. The elimination of circulating complexes containing polymeric IgA by excretion in the bile. *Immunology.* 42:83–89.
26. Potter, M. 1972. Immunoglobulin-producing tumors and myeloma proteins of mice. *Physiol. Rev.* 52:631–719.
27. Renston, R. H., A. L. Jones, W. D. Christiansen, G. T. Hradek, and B. J. Underdown. 1980. Evidence for a vesicular transport mechanism in hepatocytes for biliary secretion of immunoglobulin A. *Science (Wash. DC.).* 208:1276–1278.
28. Renston, R. H., D. G. Maloney, A. L. Jones, G. T. Hradek, K. Y. Wong, and I. D. Goldfine. 1980. Bile secretory apparatus: evidence for a vesicular transport mechanism for proteins in the rat, using horseradish peroxidase and [^{125}I] insulin. *Gastroenterology.* 78:1373–1388.
29. Roman, L. M., and A. L. Hubbard. 1983. A domain-specific marker for the hepatocyte

plasma membrane: localization of leucine aminopeptidase to the bile canalicular domain. *J. Cell Biol.* 96:1548–1558.
30. Schiff, J. M., M. M. Fisher, and B. J. Underdown. 1984. Receptor-mediated biliary transport of immunoglobulin A and asialoglycoprotein: sorting and missorting of ligands revealed by two radiolabeling methods. *J. Cell Biol.* 98:79–89.
31. Socken, D. J., K. N. Jeejeebhoy, H. Bazin, and B. J. Underdown. 1979. Identification of secretory component as an IgA receptor on rat hepatocytes. *J. Exp. Med.* 50:1538–1548.
32. Solari, R., and J.-P. Kraehenbuhl. 1984. Biosynthesis of the IgA antibody receptor: a model for the transepithelial sorting of a membrane glycoprotein. *Cell.* 36:61–71.
33. Steer, C. J., and G. Ashwell. 1980. Studies on a mammalian hepatic binding protein specific for asialoglycoproteins. Evidence for receptor recycling in isolated rat hepatocytes. *J. Biol. Chem.* 255:3008–3013.
34. Sztul, E. S., K. E. Howell, and G. E. Palade. 1983. Intracellular and transcellular transport of secretory component and albumin in rat hepatocytes. *J. Cell Biol.* 97:1582–1591.
35. Sztul, E. S., K. E. Howell, and G. E. Palade. 1985. Biogenesis of the polymeric IgA receptor in rat hepatocytes. I. Kinetic studies of its intracellular forms. *J. Cell Biol.* 100:1248–1254.
36. Sztul, E. S., K. E. Howell, and G. E. Palade. 1985. Biogenesis of the polymeric IgA receptor in rat hepatocytes. II. Localization of its intracellular forms by cell fractionation studies. *J. Cell Biol.* 100:1255–1261.
37. Takahashi, I., P. K. Nakane, and W. R. Brown. 1982. Ultrastructural events in the translocation of polymeric IgA by rat hepatocytes. *J. Immunol.* 128:1181–1187.
38. Tanabe, T., W. E. Pricer, Jr., and G. Ashwell. 1979. Subcellular membrane topology and turnover of a rat hepatic binding protein specific for asialoglycoproteins. *J. Biol. Chem.* 254:1038–1043.
39. Towbin, H., T. Staehelin, and J. Gordon. 1979. Electrophoretic transfer of proteins from polyacrylamide gels to nitrocellulose sheets: procedure and some applications. *Proc. Natl. Acad. Sci. USA.* 76:4350–4354.
40. Vaerman, J. P., and I. Lemaitre-Coelho. 1979. Transfer of circulating human IgA across the rat liver into the bile. *In* Protein Transmission through Living Membranes. W. A. Hemmings, editor. Elsevier/North-Holland Biomedical Press. 383–398.
41. Wall, D. A., G. Wilson, and A. L. Hubbard. 1980. The galactose-specific recognition system of mammalian liver: the route of ligand internalization in rat hepatocytes. *Cell.* 21:79–93.
42. Wall, D. A., and A. L. Hubbard. 1981. Galactose-specific recognition system of mammalian liver: receptor distribution on the hepatocyte cell surface. *J. Cell Biol.* 90:687–696.